

JOINING OF COMMERCIAL ALUMINIUM ALLOYS

H. K. D. H. Bhadeshia

University of Cambridge, Department of Materials Science & Metallurgy
Pembroke Street, Cambridge CB2 3QZ, U. K.
www.msm.cam.ac.uk/phase-trans

There have been quite remarkable developments in the joining of aluminium and its alloys. A few of these achievements are reviewed, including friction–stir welding, flux–free brazing, transient liquid–phase bonding using a temperature gradient, and the joining of aluminium foams.

INTRODUCTION

Aluminium forms a tenacious oxide film; it is impossible in practice to stop it from oxidising at exposed surfaces. It can nevertheless be welded because the oxide can be dispersed by the action of a welding arc [1], although fragments of oxide may become entrapped into the weld. Resistance spot welding of aluminium is difficult (though not impossible) because the oxide film can cause uncontrolled variations in surface resistance.

Unlike iron, aluminium has only one allotropic form so there are no phase transformations which can be exploited to control its microstructure. The main methods by which it can be strengthened include deformation, solution–hardening, or by introducing precipitates into the microstructure. The heat introduced by welding can severely disrupt the deformed or precipitation–hardened alloys.

FRICITION STIR WELDING

Friction stir welding [2,3] involves the joining of metals without fusion or filler materials. It is used already in routine, as well as critical applications, for the joining of structural components made of aluminium and its alloys [4,5]. Indeed, it has been convincingly demonstrated that the process results in strong and ductile joints, sometimes in systems which have proved difficult using conventional welding techniques. The process is most suitable for components which are flat and long (plates and sheets) but can be adapted for pipes, hollow sections and positional welding [3]. The welds are created by the combined action of frictional heating and mechanical deformation due to a rotating tool. The maximum temperature reached is of the order of 0.8 of the melting temperature [6].

The tool has a circular section except at the end where there is a threaded probe or more complicated flute (Fig. 1a); the junction between the cylindrical portion and the probe is known as the *shoulder*. The probe penetrates the workpiece whereas the shoulder rubs with the top surface. The heat is generated primarily by friction between a rotating–translating tool, the shoulder of which rubs against the workpiece. There is a volumetric

contribution to heat generation from the adiabatic heating due to deformation near the pin. The welding parameters have to be adjusted so that the ratio of frictional to volumetric (deformation-induced) heating decreases as the workpiece becomes thicker. This is in order to ensure a sufficient heat input per unit length. In skew-stirTM welding, the probe is inclined to the rotational-axis of the tool, enabling the volume of material swept by the probe to be increased.

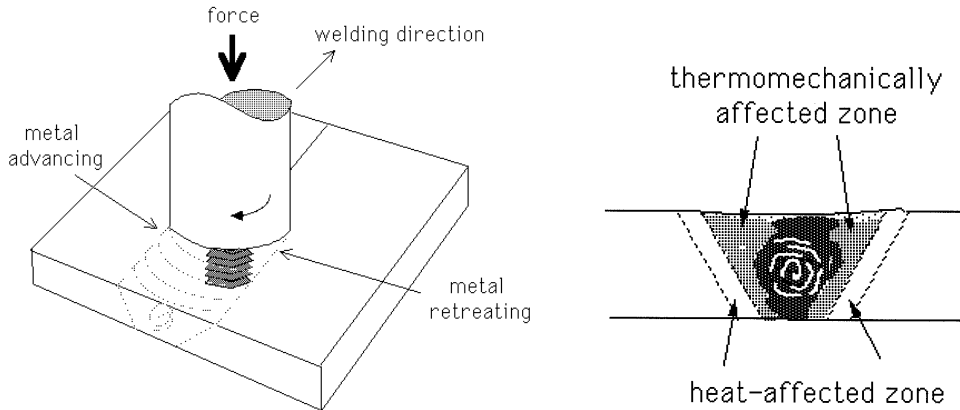


Fig. 1: Schematic illustrations: (a) tool and workpiece in friction stir welding; (b) cross-section of weld (the dark central region with the flow lines is the nugget).

Reynolds has pictured the flow of metal during friction stir welding of an aluminium alloy using embedded markers [7]; we present here a simplified view. The welding process begins when the rotating tool is plunged into the surface of the components being welded. As the tool is translated along the welding direction, the material in front is softened by frictional heating, extruded past both the sides of the pin into the cavity left as the pin advances along the welding direction. The back end of the shoulder passes over the extruded material and forges and consolidates it, leaving behind a neat weld profile. Any surface oxides which existed prior to welding are dispersed by the intense deformation.

The microstructure of a friction-stir weld depends in detail on the tool design, the rotation and translation speeds, the applied pressure and the characteristics of the material being joined. However, it can be summarised as in Fig. 1b, as consisting of a number of zones [8]. The heat-affected zone (HAZ) is as in conventional welds and is not discussed further. The central nugget region containing the onion-ring flow-pattern is the most severely deformed region, although it frequently seems to dynamically recrystallise, so that the detailed microstructure may consist of equiaxed grains. The layered (onion-ring) structure is a consequence of the way in which a threaded tool deposits material from the front to the back of the weld [9]. It seems that cylindrical sheets of material are extruded during each rotation of the tool, which on a weld cross-section give the characteristic onion-rings [10].

The thermomechanically-affected zone lies between the HAZ and nugget; the grains of the original microstructure are retained in this region, but in a deformed state. The top surface of the weld has a different microstructure, a consequence of the shearing induced

by the rotating tool–shoulder.

The friction welding tool clearly does a great deal of *redundant work* – after all, the final workpiece profile is almost identical to the original shape of the abutting components; only the bond line is eliminated by the mechanical mixing. It follows that the complete characterisation of a friction stir weld requires a knowledge of both the strain gradients and microstructure. The plastic strain gradients could in principle be measured using small samples extracted from different regions of the weld cross–section for differential scanning calorimetry. The stored energy measured in this way may provide valuable information on residual plastic strains.

The efficiency and the ability to produce good friction–stir welds depends critically on tool design [3]. Attempts are being made to develop mathematical models for tool design, although the work is at an early stage. Useful principles are nevertheless emerging. For example, it is predicted that the probe forces increase with the welding speed but decrease with the rotational speed [11].

TEMPERATURE–GRADIENT TLP BONDING

Transient liquid–phase (TLP) bonding uses a metallic interlayer, mostly in the form of thin foils, between the faying surfaces of components in a butt joint. In the case of aluminium and its alloys, the interlayer is normally a copper foil with a thickness of a few micrometers; thinner layers of copper be deposited by ion–beam sputtering. The assembly is then heated to a temperature in the vicinity of the Al–Cu eutectic temperature. The diffusion of copper into the aluminium substrate therefore induces melting, but the liquid solidifies isothermally as homogenisation occurs and the liquidus temperature rises.

Although the temporary formation of the liquid phase helps disrupt the surface–oxide layers, the oxide remains as a stable phase and is redistributed (and even concentrated) in front of the moving solid–liquid interfaces. Complete metallic contact is therefore prevented at the bond surfaces, resulting in less than optimum cohesion. The process in general leads to planar bonds, which are not ideal from the point of view of mechanical properties, particularly with respect to the resistance of the bond to shear stresses.

A remarkable variant of this process, which overcomes these difficulties, has been demonstrated by Shirzadi and Wallach [12,13,14]. The technique is known as temperature–gradient transient liquid–phase bonding (TG–TLP) because a small temperature gradient is imposed across the bond during joining. The consequence of the gradient is that the solid–liquid interface becomes unstable and adopts a convoluted shape, thereby providing mechanical keying and a better distribution of oxides and impurities at the bond. The mechanical properties, including the shear strength, then match those of the base material even when joining difficult alloys such as in the Al–Li system.

The method works as follows [15,16]. The imposition of a temperature gradient across the bond distinguishes the two liquid–solid interfaces, one of which is colder than the other (Fig. 2c). A comparison with the phase diagram (Fig. 3a,b) reveals that there is a smaller value of copper concentration in the liquid which is in equilibrium with the hot solid, *i.e.* $C_{\text{hot}}^{LS} < C_{\text{cold}}^{LS}$. It follows that there will be a transport of solute from left to right which in turn has the consequence that both the solid–liquid interfaces move in the same direction, from the cold side towards the hot side.

A more important consequence of the solute concentration gradient in the liquid is that the liquidus temperature also changes with distance (Fig. 3c). The solid–liquid interface becomes unstable to perturbations if the temperature gradient at the interface is less than the corresponding liquidus temperature gradient, as illustrated in Fig. 3c. This is because there is a constitutionally supercooled zone at the interface so that any solid–perturbation would be advancing into a undercooled melt [17,18]. It is well–known that a large consti-

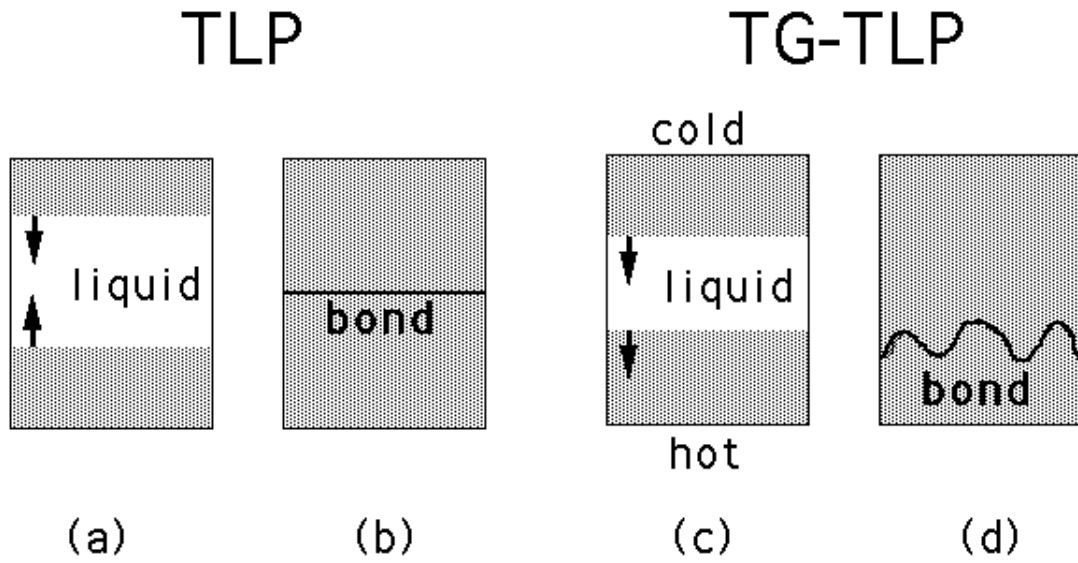


Fig. 2: A comparison of TLP and TG-TLP. (a) TLP during bonding. (b) TLP bond after completion of TLP. (c) TG-TLP during bonding. (d) Final TG-TLP bond. The arrows in (a) and (c) indicate the direction in which the solid-liquid and liquid-solid interfaces move during bonding.

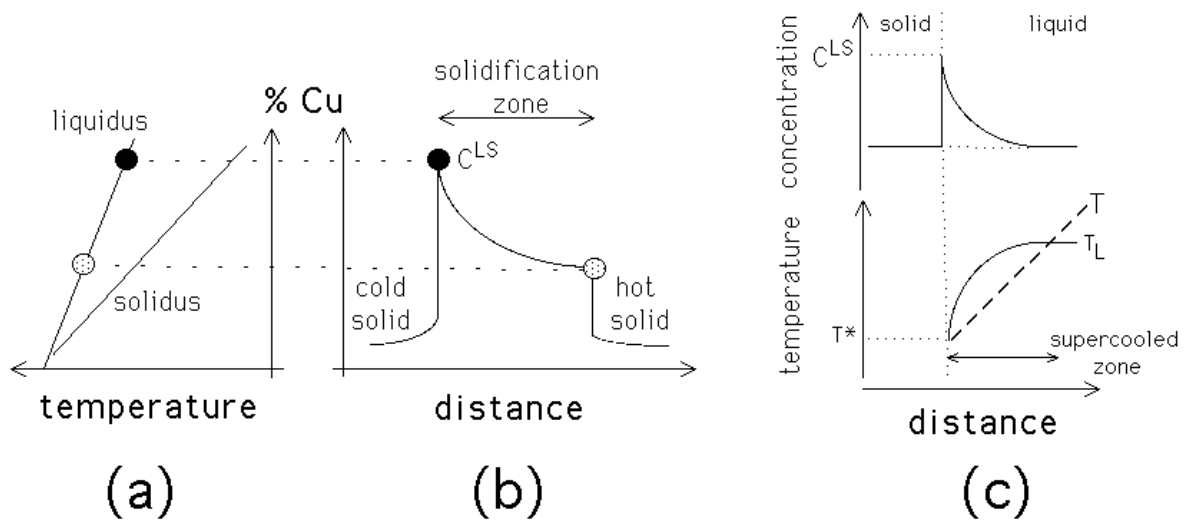


Fig. 3: (a, b) Concentration profile developed as a result of the temperature gradient in the TG-TLP process. (c) Constitutional supercooling. T is the temperature of the liquid, T_L the liquidus-temperature of the liquid, and T^* the temperature at the position of the interface.

tionally supercooled zone (Fig. 3c) leads to dendritic solidification whereas a small one is associated with the development of more gentle convolutions which do not extend large distances in the average growth direction.

Shirzadi and Wallach point out that dendritic solidification is undesirable during TG–TLP bonding because interdendritic liquid, when it solidifies, leaves behind porosity in the vicinity of the bond. A gentle, sinusoidal solidification front is, on the other hand, highly desirable when compared with a planar front, because of the keying and oxide dispersal effects mentioned earlier.

Fig. 4a, b show experiments in which the effect of the magnitude of the temperature gradient is apparent. A large gradient induces “dendritic” solidification whereas a more desirable “sinusoidal” front is obtained with a small temperature gradient. Fig. 4c, d show a comparison between TLP and TG–TLP bonded samples of Al–4Li wt% alloys; notice the planar bond line demarcated by oxide particles in the case of the TLP sample. By contrast, the TG–TLP sample has a convoluted bond surface.

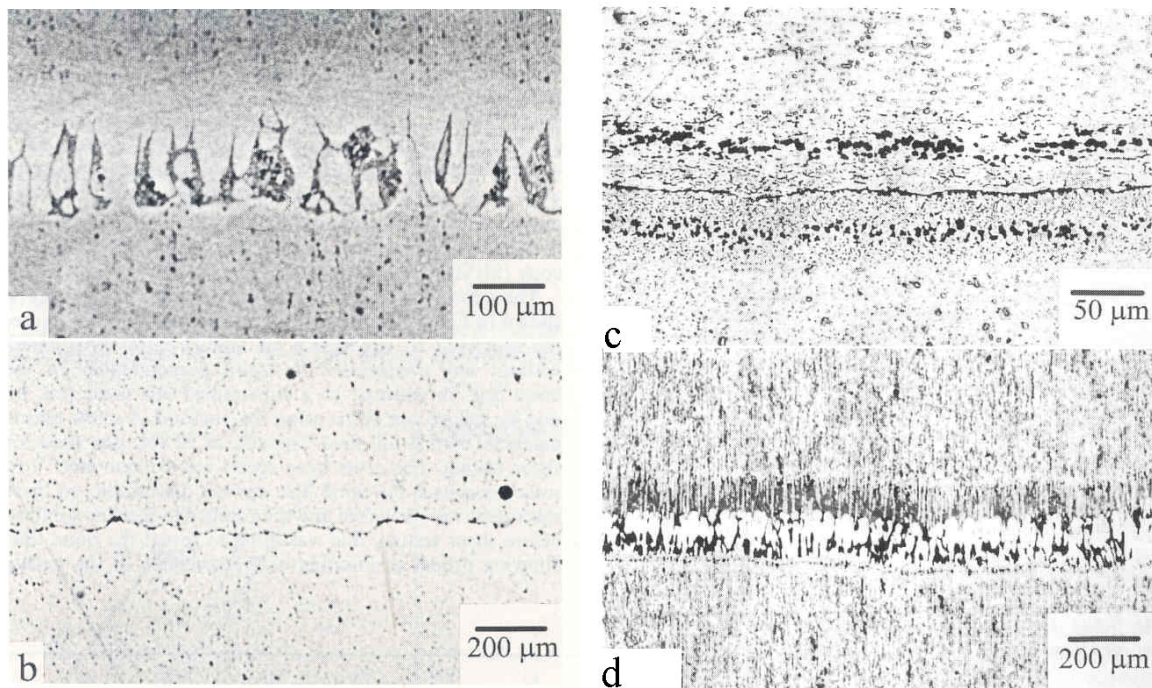


Fig. 4: Aluminium alloy (6082) TG–TLP bonded, (a) large temperature gradient; (b) small temperature gradient. Aluminium–lithium alloy, (c) TLP–bonded; (d) TG–TLP bonded. After Shirzadi and Wallach.

FLUX–FREE BRAZING

The oxide film on aluminium determines the ability to braze it; it is only with the development of fluxes which disrupt the oxide film without harming the underlying aluminium that it became possible to implement this joining method [19].

There are nevertheless, many tedious steps in the brazing procedure, including surface preparation, fluxing and the removal of fluxes which can in the long term be corrosive.

Gallium forms a eutectic liquid phase with aluminium at 29 °C and has a high solubility in aluminium. It can also disrupt the oxide film. On the other hand, it has a propensity to rapidly penetrate the grain boundaries within the aluminium, causing embrittlement (Fig. 5a). Shirzadi *et al.* [20,21] have developed a method in which a minimal quantity of gallium, about 1 mg cm⁻², is gently applied to the faying surfaces without disrupting the oxide film. The assembly is then immediately and rapidly heated to around 500 °C to allow the gallium to diffuse and homogenise into the aluminium after penetrating and disrupting the oxide. The heating process lasts no longer than 1 or 2 minutes. During bonding, the sample is subjected to a level of pressure close to the yield strength of the aluminium at the bonding temperature (\simeq 10 MPa). This produces a strong joint in which the bond position is hardly visible in an optical micrograph (Fig. 5b).

Should it be necessary to delay the heating part of the operation after applying the gallium, then it is recommended that the gallium-treated part is kept at a sub-zero temperature in order to prevent it from attacking the grain boundaries in the aluminium.

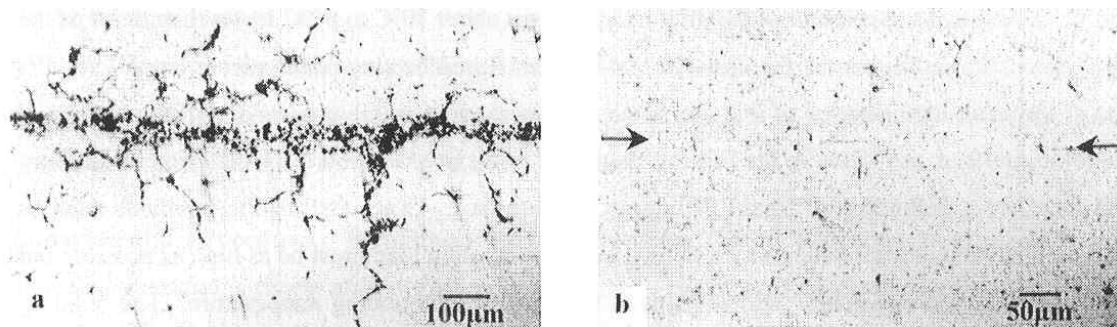


Fig. 5: Pure aluminium, (a) bonded by rubbing gallium on the faying surfaces to disrupt the oxide; (b) bond achieved using minimal quantity of gallium applied gently (arrows indicate position of bond). After Shirzadi *et al.*[21].

ALUMINIUM FOAMS

Metallic foams containing as much as 90% porosity are of interest primarily because of their low density (leading to a high stiffness-to-weight ratio), in mechanical damping including acoustic absorption and in thermal management [22,23]. A popular method for making aluminium foam is by compacting the powdered metal with TiH₂ which is a foaming-agent, and then heating this compact in a furnace, at a temperature close to the melting point of the aluminium alloy. The gas released from the decomposition of the TiH₂ causes expansion into a closed-cell foam with a porosity that can be controlled in the range 60–85% [24].

There has been substantial progress in the joining of aluminium foams using laser welding [25]; the work covers both the joining of foams to foams and to ordinary metals. A laser has the particular advantage that the hot zone is narrow, thereby ensuring as little structural damage to the foam as is possible.

Nevertheless, the problem with any fusion welding process is that the foam collapses on melting, leaving behind a pool which is much smaller than the original volume of the unmelted foam. The weld therefore has to be made using filler materials (Fig. 6). One option is to use a conventional filler-rod supplied at a rate which compensates for the

volume shrinkage (Fig. 6a) but the welding speed is then limited by the ability of the laser to melt the filler. The use of a thin filler-sheet (Fig. 6b) allows a higher welding speed to be achieved. However, to achieve a porous weld requires the use of foamable profile (Fig. 6d) or a paste filler which contains the foaming agent TiH_2 (Fig. 6d). An alternative is to use a gaseous filler by injecting an inert gas from the bottom surface.

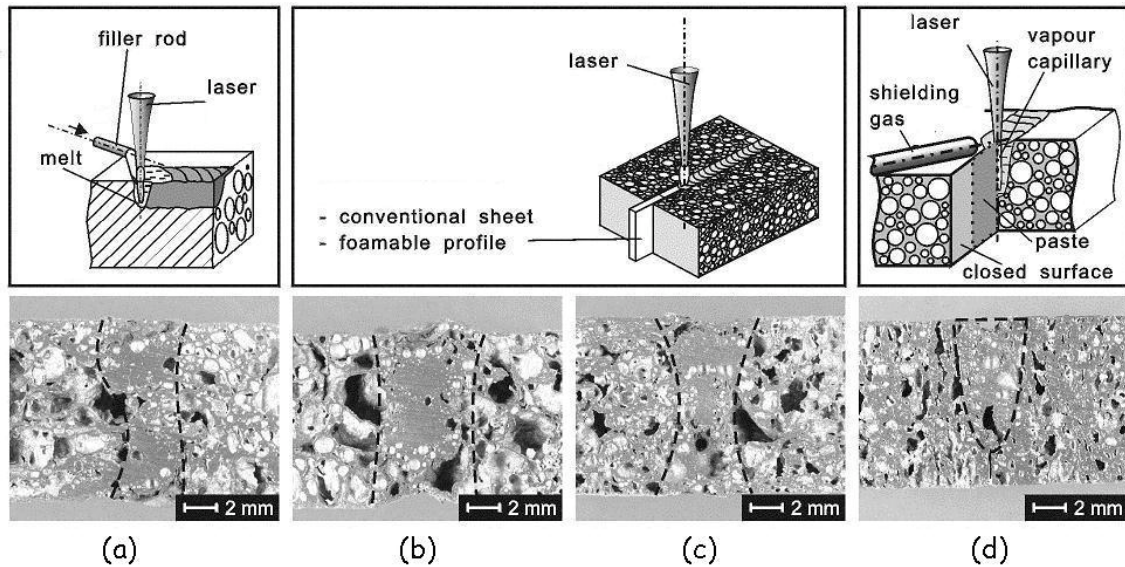


Fig. 6: Cross-sections of laser-welded aluminium foam using different filler materials: (a) filler rod; (b) conventional sheet; (c) foamable sheet; (d) foam-generating paste. [25]

NOVEL EXPERIMENTAL TECHNIQUE

Many aluminium alloys are susceptible to hot-cracking in circumstances where the system acquires mechanical strength before it has ductility. Hot-cracking is sensitive to the chemical composition, partly because the latter also determines the freezing range. The conventional way of studying the tendency for cracking as a function of the composition is to make and test several different alloys.

Dahan *et al.* [26] have designed an experimental method which removes much of the tedium associated with such work. By making a wedge shaped composite of two different alloys, a single sample can be used to study the cracking behaviour as a function of composition. The latter is varied simply by locating welds at many positions along the horizontal axis, as illustrated in Fig. 7.

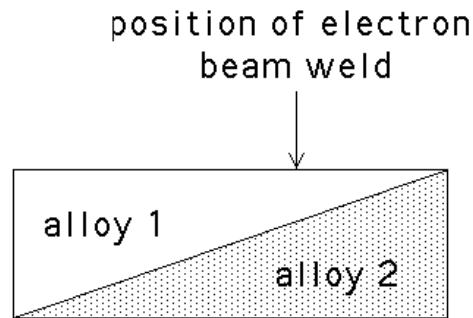


Fig. 7: Composite alloy. The weld position can be varied along the horizontal direction to select a specific chemical composition.

SUMMARY

It is heartening that there have been so many ingenious developments in the joining of both ordinary aluminium alloys, which form the backbone of the industry, and in the bonding of niche materials such as the aluminium foams. And this has all been achieved in spite of the pernicious oxide film!

ACKNOWLEDGMENTS

I am grateful to Professors K. S. S. Murthy and D. Sastry for the opportunity of presenting this paper. I would also like to thank the Governing Council of the Indian Institute of Science, Bangalore, and the Indian Aluminium Company of Calcutta, for the *Aditya Birla Chair*. I have greatly enjoyed reading the papers by Shirzadi and co-workers.

REFERENCES

1. J. F. Lancaster: *Metallurgy of Welding, Brazing and Soldering*, 2nd edition, Institution of Metallurgists, London (1970) 217–227.
2. W. M. Thomas, E. D. Nicholas, J. C. Needham, M. G. Nurch, P. Temple-Smith and C. Dawes: *Patents on friction stir butt welding* (1991–1995) International: PCT/GB92/02203; British: 9125978.8; USA: 5460317.
3. W. M. Thomas and R. E. Dolby: *6th Int. Trends in Welding Research Conference*, ASM Int., eds S. A. David, T. DebRoy, J. C. Lippold, H. B. Smartt and J. M. Vitek (2003) 203–211.
4. E. D. Nicholas and W. M. Thomas: *Int. Journal of Materials & Product Technology* **13** (1998) 45–55.
5. W. M. Thomas, E. D. Nicholas: *Materials & Design* **18** (1997) 269–273.
6. W. Tang, X. Guo, J. C. McClure and L. E. Murr: *Journal of Materials Processing & Manufacturing Science* **7** (1999) 163–172.
7. A. P. Reynolds: *Science and Technology of Welding and Joining* **5** (2000) 120–124.
8. H. R. Shercliff and P. A. Colegrove: *Mathematical Modelling of Weld Phenomena 6*, Maney Publishing, London, eds H. Cerjak and H. K. D. H. Bhadeshia (2002) 927–974.
9. K. Colligan: *Welding Journal Research Supplement* **78** (1999) 229s–337s.
10. K. N. Krishnan: *Materials Science and Engineering* **327** (2002) 246–251.
11. P. Ulysse: *Int. Journal of Machine Tools & Manufacture* **42** (2002) 1549–1557.

12. A. A. Shirzadi and E. R. Wallach: *Science and Technology of Welding and Joining* **2** (1997) 89–94.
13. A. A. Shirzadi and E. R. Wallach: *U.K. patent 9709167.2* (1997)
14. A. A. Shirzadi: *Ph.D. thesis*, University of Cambridge, U. K. (1998)
15. A. A. Shirzadi and E. R. Wallach: *Acta Materialia* **47** (1999) 3551–3560.
16. H. Assadi, A. A. Shirzadi and E. R. Wallach: *Acta Materialia* **49** (2001) 31–39.
17. J. W. Rutter and B. Chalmers: *Canadian J. of Physics* **31** (1953) 15.
18. J. W. Christian: *Theory of Transformations in Metals and Alloys*, Part II, 3rd edition, Pergamon Press, Oxford (2002)
19. ASM: *Metals Handbook*, 9th edition, American Society for Metals, USA **6** (1983) 1022–1032.
20. A. A. Shirzadi, G. Saindrenan and E. R. Wallach: *Materials Science Forum* **396–402** (2002) 1579–1584.
21. A. A. Shirzadi and G. Saindrenan: *Science and Technology of Welding and Joining* (2003) in press.
22. M. F. Ashby, A. G. Evans, N. A. Fleck, L. J. Gibson, J. W. Hutchinson and H. N. G. Wadley: *Metal Foams: A Design Guide*, Butterworth Heinemann, Oxford (2000)
23. J. Banhart: *Progress in Materials Science* **46** (2001) 491–496.
24. S. Amjad: *M.Phil. Thesis*, University of Cambridge (2002)
25. H. Haferkamp, J. Bunte, D. Herzog and A. Ostendorf: *Science and Technology of Welding and Joining* (2003) in press.
26. I. Dahan, E. Dabush, A. Stern and D. Eilliezer: *6th Int. Trends in Welding Research Conference*, ASM Int., eds S. A. David, T. DebRoy, J. C. Lippold, H. B., Smartt and J. M. Vitek (2003) 672–675.